Cooperative Interference Mitigation Using Fractional Frequency Reuse and Intercell Spatial Demultiplexing

Jaewon Chang, Jun Heo, and Wonjin Sung

Abstract: **For mobile wireless systems with full frequency reuse, co-channel interference near the cell coverage boundaries has a significant impact on the signal reception performance. This paper addresses an approach to efficiently mitigate the effect of downlink co-channel interference when multi-antenna terminals are used in cellular environments, by proposing a signal detection strategy combined with a system-level coordination for dynamic frequency reuse. We demonstrate the utilization of multi-antennas to perform spatial demultiplexing of both the desired signal and interfering signals from adjacent cells results in significant improvement of spectral efficiency compared to the maximal ratio combining (MRC) performance, especially when an appropriate frequency reuse based on the traffic loading condition is coordinated among cells. Both analytic expressions for the capacity and experimental results using the adaptive modulation and coding (AMC) are used to confirm the performance gain. The robustness of the proposed scheme against varying operational conditions such as the channel estimation error and shadowing effects are also verified by simulation results.**

Index Terms: **Co-channel interference, fractional frequency reuse, interference mitigation, maximal ratio combining, spatial demultiplexing.**

I. INTRODUCTION

In typical cellular mobile radio systems, co-channel interference is one of the critical factors which determine the performance of signal detection. The co-channel interference degrades the link quality, and decreases the system bandwidth efficiency as well as the fairness of the service. To overcome this weakness in cellular operation, interference mitigation methods have been widely investigated and developed for various systems including recent standards such as the IEEE802.16e Mobile WiMAX [1]–[3].

The effect of co-channel interference has been analyzed by considering various statistical characteristics of the wireless channel and system conditions, including the short-term fading, log-normal shadowing, and network loading [4]–[10], which suggests the performance impairment near coverage boundaries remains substantial even when optimum signal combining [11] is used. In an effort to reduce the performance degradation, a number of approaches for the co-channel interference coordination and mitigation have been proposed. For the interference coordination, the dynamic channel allocation strategy was first suggested in [12], [13], and the channel assignment using frequency reuse is investigated in [14]. While decreasing the frequency reuse factor significantly reduces the amount of interference from adjacent cells, a pre-determined reuse factor does not always maximize the overall system capacity. To further enhance the efficiency of frequency utilizations, fractional frequency reuse (FFR) has recently been proposed by Qualcomm [15]. The FFR scheme adaptively changes the frequency reuse factor based on the link quality experienced by mobile stations (MS), to improve the spectral efficiency at the expense of the system operational complexity.

In this paper, we propose a cooperative interference mitigation method when MS's with multiple receive antennas are used for the SIMO downlink channel in multi-cell environments. By performing *intercell spatial demultiplexing* (ISD) when the MS is located at regions with strong interference from adjacent cells, we demonstrate the spectral efficiency of the system can be significantly improved compared to the performance of MRC. In particular, we show the effectiveness of proposed ISD is further enhanced when the scheme is synergetically combined with the FFR operation. Using both analytic and experimental results, we present operation scenarios for the system-level cooperation for the FFR as well as the detection strategy of the receiver. For all numerical evaluation of the proposed scheme, transmission parameters for the IEEE802.16e standard [3] with AMC are used. Practical aspects of the operation are also considered, including the effects of the channel estimation accuracy, traffic loading, and shadowing of the wireless channel.

The organization of the paper is as follows. The descriptions for the signal model and the FFR scheme in multi-cell environments are given in Section II, and the performance of ISD in terms of the effective signal-to-interference plus noise ratio (SINR) and the normalized capacity is analyzed for different frequency reuse factors in Section III, where the comparison with the conventional MRC detection is also given. Section IV contains the performance evaluation of the proposed scheme using the AMC-based link adaptation method to confirm the analytic results, followed by discussion on practical considerations in Section V which also includes investigation results on potential extension of the scheme to systems with multi-antenna base stations (BS). Conclusions are given in Section VI.

II. SYSTEM MODEL

A. Received Signal in Multi-cell Environment

We consider the downlink transmission from the single-antenna BS to the target MS equipped with N antennas as shown in Fig. 1. We assume BS_1 transmits the desired signal while other BS's transmit interfering signals to the MS. The received

Manuscript received November 18, 2007.

J. Chang and W. Sung are with the Department of Electronic Engineering, Sogang University, 1 Sinsu-dong, Mapo-gu, Seoul 121-742 Korea, email: {cygnus6, wsung}@sogang.ac.kr.

J. Heo is with the School of Electrical Engineering, Korea University, 1 Anam-dong 5-ga, Seongbuk-gu, Seoul 136-701 Korea, email: junheo@korea.ac.kr.

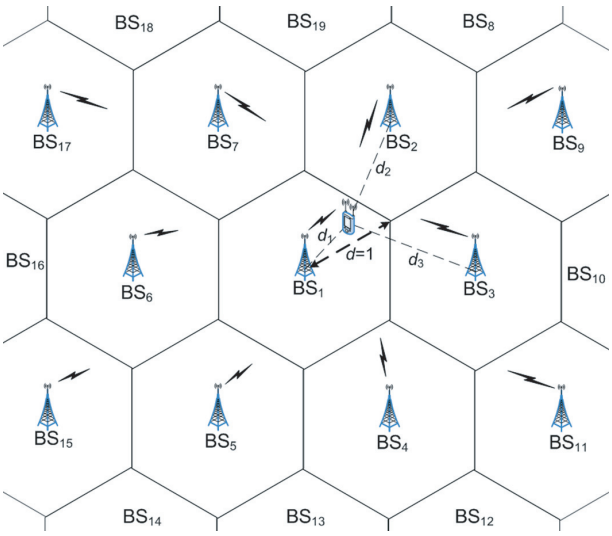

Fig. 1. Transmission model in a multi-cell environment.

signal power at the MS from BS_i can be written as [16]

$$P_i = PL_i d_i^{-\gamma} \tag{1}$$

where P is the transmit power and L_i represents the effect of shadowing in the wireless channel. Also, d_i is the distance from the BS_i to the MS and γ is the pathloss exponent. The received signal vector $\mathbf{r} = [r_1, \cdots, r_N]^T$ consisting of the desired signal component from the home BS, the interfering signal components from BS's of adjacent cells, and the thermal noise component is given by

$$\mathbf{r} = \sqrt{P_1}\mathbf{h}_1 s_1 + \sum_{i \in I} \sqrt{P_i}\mathbf{h}_i s_i + \mathbf{n} \tag{2}$$

where I denotes the set of indices for the BS's transmitting interference signals, s_i is the transmission symbol with normalized power $\mathbb{E}[|s_i|^2] = 1$, and $\mathbf{h}_i = [h_{i,1}, \cdots, h_{i,N}]^T$ is the SIMO channel vector from BS_i to the MS. Components $\{h_{ij}\}$ are uncorrelated complex Gaussian with unit variance, which represent the independent Rayleigh fading channel. Noise vector $\mathbf{n} = [n_1, \cdots, n_N]^T$ is composed of $\{n_j\}$ which are uncorrelated complex Gaussian with variance σ_n^2. Denoting the weight vector for signal combining at the MS by $\mathbf{w} = [w_1, \cdots, w_N]$ with the normalized power $|\mathbf{w}|^2 = 1$, the receiver output after combining is

$$y = \mathbf{w}\mathbf{r}. \tag{3}$$

The instantaneous effective SINR of the receiver, following the definition in [17] and [18, p. 122], can be written as

$$\mu = \frac{P_1|\mathbf{w}\mathbf{h}_1|^2}{\sigma_I^2 + \sigma_w^2} \tag{4}$$

where $\sigma_I^2 = \mathbb{E}[\sum_{i \in I} P_i|\mathbf{w}\mathbf{h}_i|^2]$ is the interference signal power and $\sigma_w^2 = \mathbb{E}[|\mathbf{w}\mathbf{n}|^2] = \sigma_n^2$ is the power of weighted noise. The weight vector is determined from the channel state information, which is assumed to be accurately estimated at the receiver unless otherwise stated.

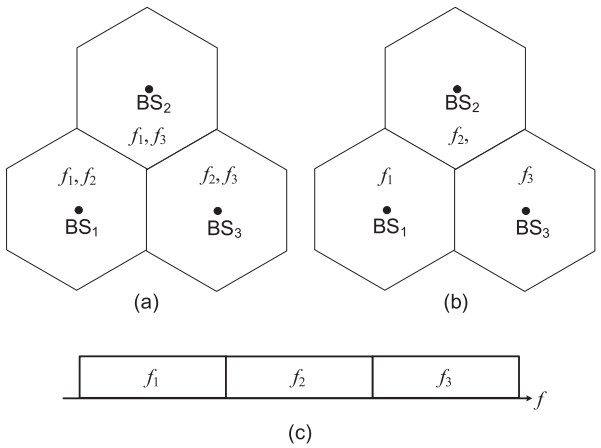

Fig. 2. Resource allocation for the frequency reuse: (a) Frequency reuse factor of $r = 2/3$, (b) frequency reuse factor of $r = 1/3$, and (c) channelization of the bandwidth.

B. Fractional Frequency Reuse

Frequency reuse is often used in interference limited systems to improve the link reliability, especially near the cell coverage boundaries. Frequency reuse involves partitioning the available bandwidth into multiple portions, and assigning different portions to neighboring cells (or sectors) to minimize the out-of-cell interference. All MS's within a cell can only use the portion of the bandwidth assigned to that cell. Despite the improved link quality for users with low SINR, small values of frequency reuse usually result in a reduced overall spectral efficiency in a cell. FFR is a bandwidth reuse scheme with reduced resource overhead compared to conventional frequency reuse. Each MS can be assigned a partial bandwidth with various reuse factors depending on the link quality, in comparison to the common frequency bandwidth with a fixed reuse factor for the conventional frequency reuse.

Fig. 2 shows the frequency resource assignment for three adjacent cells. For the reuse factor $r = 2/3$ of Fig. 2(a), each BS is assigned with 2/3 portions of the whole bandwidth, resulting in a reduced amount of co-channel interference. BS_1 using two frequency blocks denoted as f_1 and f_2 in Fig. 2(c) shares the f_1 block with BS_2, and shares the f_2 block with BS_3. Further reduction of the interference from adjacent cells occurs when the reuse factor decreases to $r = 1/3$ as shown in Fig. 2(b). Frequency blocks f_1, f_2, and f_3 are disjointly assigned to BS_1, BS_2, and BS_3, with no neighboring cells using a common bandwidth resource. For the remainder of discussion, we consider a cellular system based on FFR which dynamically changes its reuse factor among $r = 1, 2/3$, and $1/3$ for the enhanced performance. More specifically, we demonstrate an improved system spectral efficiency is achieved by combining an appropriate value of r with the ISD scheme, when compared to the MRC detection with any values of frequency reuse factor.

III. SIGNAL DETECTION

A. Conventional MRC

Signal detection using MRC is the optimal diversity scheme to maximize the output SINR of the receiver for the noise-

limited channel [19]. When the signals at multiple receive antennas are maximal ratio combined, the output signal using the weight vector $\mathbf{w} = \mathbf{h}_1^H/|\mathbf{h}_1|$ matched to the channel from BS_1 is

$$\begin{aligned} y_{\text{MRC}} &= \mathbf{wr} \\ &= \sqrt{P_1}\mathbf{w}\mathbf{h}_1 s_1 + \sum_{i\in I}\sqrt{P_i}\mathbf{w}\mathbf{h}_i s_i + \mathbf{wn} \end{aligned} \tag{5}$$

where $[\cdot]^H$ is the Hermitian operator. The effective SINR of the MRC signal detection is given by

$$\mu = \frac{P_1|\mathbf{w}\mathbf{h}_1|^2}{\sigma_I^2 + \sigma_n^2} = \rho_{\text{MRC}}|\mathbf{h}_1|^2 \tag{6}$$

where we defined

$$\rho_{\text{MRC}} = \frac{P_1}{\sigma_I^2 + \sigma_n^2}. \tag{7}$$

The effective SINR is chi-square distributed with $2N$ degrees of freedom [20], with the corresponding probability density function (pdf)

$$f(\mu) = \frac{1}{\Gamma(N)\rho_{\text{MRC}}^N}\mu^{N-1}\exp\left(-\frac{\mu}{\rho_{\text{MRC}}}\right),\ \mu \geq 0 \tag{8}$$

where $\Gamma(\cdot)$ is the gamma function. The average value $\bar{\mu}_{\text{MRC}}$ of the effective SINR is determined as

$$\bar{\mu}_{\text{MRC}} = N\rho_{\text{MRC}}. \tag{9}$$

The factor N obtained from $\mathbb{E}[|\mathbf{h}_1|^2] = N$ represents the array gain of the MRC detection.

From the capacity formula, the average value of the capacity in the unit of bps/Hz, normalized by the bandwidth and reuse factor r is obtained from the expression

$$\eta = r\int_0^\infty \log_2(1+\mu)f(\mu)d\mu. \tag{10}$$

Multiplication by r reflects the reduced amount of bandwidth assignment for transmission from the BS. Combining (8) and (10), we derive the normalized capacity for the MRC detection at a given location of the MS as

$$\eta_{\text{MRC}} = \frac{r}{\Gamma(N)\rho_{\text{MRC}}^N}\int_0^\infty \mu^{N-1}\log_2(1+\mu)\exp\left(-\frac{\mu}{\rho_{\text{MRC}}}\right)d\mu. \tag{11}$$

By evaluating the integral, we obtain a closed-form expression of the capacity for the dual antenna case ($N = 2$) as

$$\eta_{\text{MRC}} = r \times \frac{\rho_{\text{MRC}} + (1-\rho_{\text{MRC}})\exp\left(\frac{1}{\rho_{\text{MRC}}}\right)\text{Ei}\left[-\frac{1}{\rho_{\text{MRC}}}\right]}{(\ln 2)\rho_{\text{MRC}}} \tag{12}$$

where $\text{Ei}[u] = -\int_{-u}^{\infty} e^{-v}/v\, dv$ is the exponential integral function.

B. Intercell Spatial Demultiplexing

In conventional centralized MIMO systems, a BS equipped with N antennas can transmit up to N independent data streams for spatial multiplexing transmission. At the receiver side, an MS with N receive antennas performs spatial demultiplexing which eliminates multistream interference to recover the transmitted data streams. Various methods exist for such receiver processing for data detection, including the zero-forcing (ZF), minimum mean-square-error (MMSE) [21], ZF-SIC (V-BLAST) [22], and MMSE-SIC [23] algorithms. For example, the weight matrix for the ZF method is given by

$$\mathbf{W} = (\mathbf{G}_1^H\mathbf{G}_1)^{-1}\mathbf{G}_1^H \tag{13}$$

where $\mathbf{G}_1$ is the $N \times N$ MIMO channel matrix for the channel between the home BS (BS_1) and the MS. The weight matrix is multiplied to the received signal vector to obtain the output signal vector of the ZF receiver

$$\mathbf{y} = \mathbf{W}\mathbf{G}_1\mathbf{s}_1 + \mathbf{W}\left(\sum_{i\neq 1}\mathbf{G}_i\mathbf{s}_i + \mathbf{n}\right) \tag{14}$$

where $\mathbf{s}_i = [s_{i,1}, s_{i,2}, \cdots, s_{i,N}]^T$ is the multistream data vector from BS_i, matrix $\mathbf{G}_i$ represents the channel from BS_i to the MS. For detection of the kth substream data symbol from BS_1, the kth row vector $\mathbf{w}_k$ of the weight matrix is multiplied to the received signal vector $\mathbf{r}$. As described in [24], $\mathbf{w}_k$ works as the nulling vector for the interfering substreams from the same BS and satisfies the relation

$$\mathbf{w}_k[\mathbf{G}_1]_j = \begin{cases} 0, & j \neq k \\ 1, & j = k \end{cases} \tag{15}$$

where $[\mathbf{G}_1]_j$ is the jth column of $\mathbf{G}_1$. The corresponding signal model is represented as

$$\begin{aligned} y_k &= \mathbf{w}_k\mathbf{G}_1\mathbf{s}_1 + \mathbf{w}_k\left(\sum_{i\neq 1}\mathbf{G}_i\mathbf{s}_i + \mathbf{n}\right) \\ &= s_{1,k} + \sum_{i\neq 1}\mathbf{w}_k\mathbf{G}_i\mathbf{s}_i + \mathbf{w}_k\mathbf{n}. \end{aligned} \tag{16}$$

This type of spatial demultiplexing can also be applied to our system in consideration for nulling of adjacent cell interference signals, for which N BS's with a single transmit antenna and the MS with N receive antennas form the distributed MIMO channel. By modeling the channel between the geographically spread transmit antennas of different BS's and multiple antennas of the MS as a distributed MIMO channel, the spatial demultiplexing operation is performed to detect the desired signal as well as $N-1$ strongest interference signals. Similar to spatial demultiplexing for the centralized MIMO channel, the effects of $N-1$ strongest interference signals from adjacent cells are nullified and the data stream from BS_1 is recovered. Such operation is referred to as intercell spatial demultiplexing. ISD operations using the ZF and MMSE algorithms for spatial demultiplexing are respectively called ZF-ISD and MMSE-ISD.

B.1 ZF-ISD

Let $I_0 = \{i_1, i_2, \cdots, i_{N-1}\}$ denote the set of indices for the BS's transmitting $N-1$ strongest interference signals to the MS, and let $I_1 \triangleq I \setminus I_0$ (i.e., $I_0 \cup I_1 = I$). Thus I_1 is the set of indices for the BS transmitting interference signals which are not nullified by the ISD receiver. For example, suppose the strongest interfering signal for the MS with $N = 2$ antennas in the 19-cell model of Fig. 1 is received from BS_2. When the full frequency reuse ($r = 1$) is used, the sets become $I_0 = \{2\}$ and $I_1 = \{3, 4, \cdots, 19\}$. We also define N-dimensional symbol vector $\mathbf{s} = [s_1, s_{i_1}, s_{i_2}, \cdots, s_{i_{N-1}}]^T$, and $N \times N$ channel matrix

$$\mathbf{H} = \left[\sqrt{P_1}\mathbf{h}_1 \sqrt{P_{i_1}}\mathbf{h}_{i_1} \sqrt{P_{i_2}}\mathbf{h}_{i_2} \cdots \sqrt{P_{i_{N-1}}}\mathbf{h}_{i_{N-1}}\right].$$

Then the received signal in (2) can be rewritten as

$$\begin{aligned}\mathbf{r} &= \sqrt{P_1}\mathbf{h}_1 s_1 + \sum_{i\in I_0} \sqrt{P_i}\mathbf{h}_i s_i + \sum_{i\in I_1} \sqrt{P_i}\mathbf{h}_i s_i + \mathbf{n} \\ &= \mathbf{H}\mathbf{s} + \sum_{i\in I_1} \sqrt{P_i}\mathbf{h}_i s_i + \mathbf{n}. \end{aligned} \tag{17}$$

Matrix $\mathbf{H}$ represents the distributed MIMO channel for the desired and $N-1$ interfering data streams. For the ZF-ISD operation, weight matrix $\mathbf{W}$ is obtained from the pseudo-inverse of $\mathbf{H}$ as

$$\mathbf{W} = (\mathbf{H}^H\mathbf{H})^{-1}\mathbf{H}^H = \begin{bmatrix} \mathbf{w}_1 \\ \vdots \\ \mathbf{w}_N \end{bmatrix}. \tag{18}$$

For the detection of the desired signal using ZF-ISD, the first row vector with power normalization $\mathbf{w} = \mathbf{w}_1/|\mathbf{w}_1|$ is used to combine the received signal as

$$y_{\text{ISD}} = \mathbf{w}\mathbf{r}. \tag{19}$$

The corresponding effective SINR is given by

$$\mu = \frac{P_1|\mathbf{w}\mathbf{h}_1|^2}{\sigma_{I_1}^2 + \sigma_n^2} = \rho_{\text{ISD}}|h|^2 \tag{20}$$

where $\sigma_{I_1}^2 = \mathbb{E}[\sum_{i\in I_1} P_i|\mathbf{w}\mathbf{h}_i|^2]$ is the power of interference signals which are not separated using ZF-ISD, $h = \sum_{j=1}^{N} w_j h_{i,j}$ is the weighted channel response as described in [25] for the ZF detection, and ρ_{ISD} is defined as

$$\rho_{\text{ISD}} = \frac{P_1}{\sigma_{I_1}^2 + \sigma_n^2}. \tag{21}$$

The effective SINR for the signal detection using ZF-ISD follows the exponential distribution with the pdf

$$f(\mu) = \frac{1}{\rho_{\text{ISD}}}\exp\left(-\frac{\mu}{\rho_{\text{ISD}}}\right),\ \mu \geq 0. \tag{22}$$

Since $\mathbb{E}[|h|^2] = 1$, the effective SINR for the signal detection using ZF-ISD has the average

$$\bar{\mu}_{\text{ZF-ISD}} = \rho_{\text{ISD}}. \tag{23}$$

Combining (10) and (22), a closed-form expression of the capacity using ZF-ISD is obtained as

$$\begin{aligned}\eta_{\text{ZF-ISD}} &= r\int_0^\infty \log_2(1+\mu) f(\mu) d\mu \\ &= -\frac{r\exp\left(\frac{1}{\rho_{\text{ISD}}}\right)\text{Ei}\left[-\frac{1}{\rho_{\text{ISD}}}\right]}{\ln 2}. \end{aligned} \tag{24}$$

B.2 MMSE-ISD

For ISD using the MMSE algorithm, the weight matrix $\mathbf{W}$ is determined as

$$\mathbf{W} = (\mathbf{H}^H\mathbf{H} + \sigma_n^2\mathbf{I})^{-1}\mathbf{H}^H. \tag{25}$$

To detect the desired signal, the first row vector with power normalization $\mathbf{w} = \mathbf{w}_1/|\mathbf{w}_1|$ is multiplied to the received signal vector. Since the MMSE detection is equivalent to optimum combining [23, Appendix A], the effective SINR for the MMSE algorithm follows the chi-square distribution with $2N$ degrees of freedom

$$f(\mu) = \frac{1}{\Gamma(N)\rho_{\text{ISD}}^N}\mu^{N-1}\exp\left(-\frac{\mu}{\rho_{\text{ISD}}}\right),\ \mu \geq 0. \tag{26}$$

as shown in [26], and this result for the centralized MIMO directly applies to MMSE-ISD as well. The corresponding average SINR is

$$\bar{\mu}_{\text{MMSE-ISD}} = N\rho_{\text{ISD}}. \tag{27}$$

Combining (10) and (26), a closed-form expression of the capacity for the dual antenna case ($N = 2$) using MMSE-ISD is obtained as

$$\eta_{\text{MMSE-ISD}} = r \times \frac{\rho_{\text{ISD}} + (1-\rho_{\text{ISD}})\exp\left(\frac{1}{\rho_{\text{ISD}}}\right)\text{Ei}\left[-\frac{1}{\rho_{\text{ISD}}}\right]}{(\ln 2)\rho_{\text{ISD}}}. \tag{28}$$

C. Comparison

The effective SINR and the capacity for the MRC, ZF-ISD, and MMSE-ISD detection schemes are compared using the 19-cell system model in Fig. 1 with frequency reuse factors $r = 1$, 2/3, and 1/3. The Rayleigh flat fading channel with the pathloss exponent $\gamma = 3.76$ suggested in [27] is used for the numerical evaluation, and the effects of shadowing and thermal noise are assumed negligible. For performance evaluation, we assume the dual-antenna ($N = 2$) MS is uniformly located on a ring of radius d as shown in Fig. 3, where d is the normalized distance ranging from 0 (cell center) to 1 (hexagonal vertex). The effective SINR and normalized capacity values are calculated for incremental values of angle θ shown in the figure, which are averaged over all angles to represent the performance at given values of d.

The average effective SINRs calculated using (9), (23), and (27) are plotted in Fig. 4 for the case of full frequency reuse ($r = 1$). The effective SINR of ZF-ISD becomes greater than that of MRC as the MS moves away from the cell center, and the SINR gain using ZF-ISD over MRC is about 2 dB at the cell edge

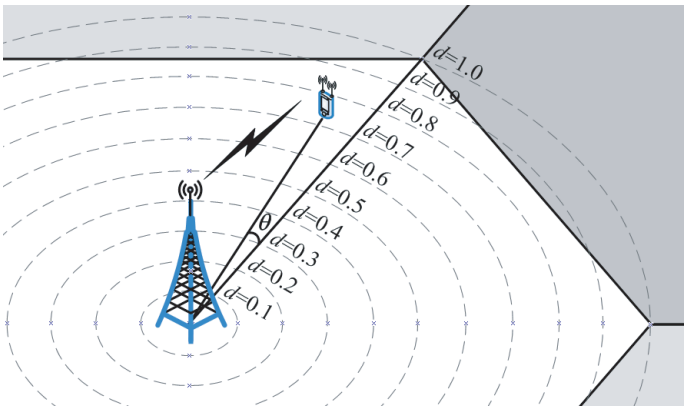

Fig. 3. Concentric rings for the performance evaluation, with radii equal to varying normalized distances from the home BS to the target MS.

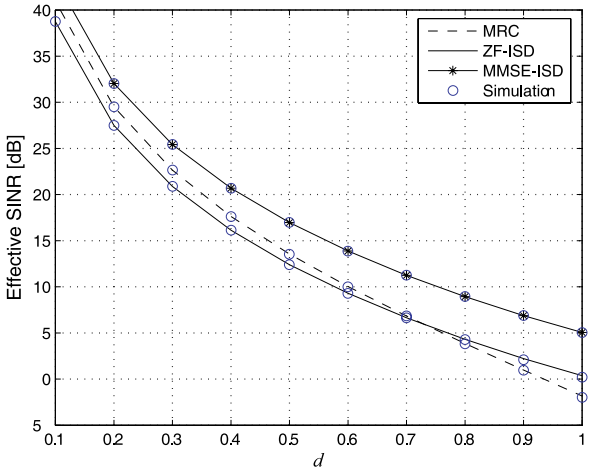

Fig. 4. Location-wise average effective SINR using MRC, ZF-ISD, and MMSE-ISD for reuse factors $r = 1$.

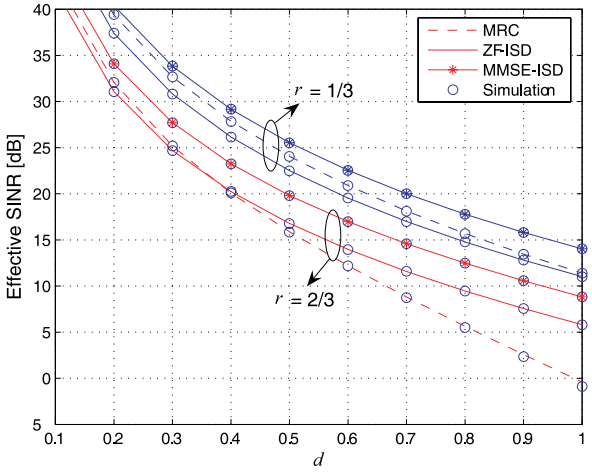

Fig. 5. Location-wise average effective SINR using MRC and ZF-ISD, and MMSE-ISD for reuse factors $r = 1/3$ and $2/3$.

$(d = 1)$. A further improvement in SINR is achieved by using MMSE-ISD, which significantly outperforms both the MRC and ZF-ISD over the entire range of the normalized distance. The gain obtained from using MMSE-ISD over MRC amounts to 7 dB at the cell edge. A similar performance behavior is also shown in Fig. 5 for reduced reuse factors $r = 2/3$ and $r = 1/3$. In general, SINR values tend to increase as the reuse factors decrease due to the reduced amount of interference. For all reuse factor values, MMSE-ISD exhibits the highest effective SINR over the entire cell region. The gain of MMSE-ISD over MRC is most dramatic for the case of $r = 2/3$. This is because two significant signal components exist near the cell edge when the reuse factor is 2/3, and ISD using dual antennas is capable of separating two data streams. Increasing the number of antennas enhances the demultiplexing capability of the receiver near cell boundaries by nullifying more interference data streams. The results determined from analytic formulas are also verified by the simulation results shown in symbol 'o' in the figures, which are obtained from separate power measurements of the desired and interference signal components.

From the effective SINR expressions in (6) and (20), we observe the advantage of MRC is the array gain of N due to the signal combining matched to the channel, while the advantage of ISD is the reduced amount of interference by removing the signal components for the BS's with indices in I_0. Ignoring the thermal noise, the average effective SINRs for MRC and ZF-ISD become identical when

$$\frac{N}{\sigma_{I_0}^2 + \sigma_{I_1}^2} = \frac{1}{\sigma_{I_1}^2} \tag{29}$$

and this is equivalent to the relation $(N-1)\sigma_{I_1}^2 = \sigma_{I_0}^2$. Using the distance parameter, the average effective SINRs of MRC and ZF-ISD become equal at a location satisfying the condition

$$(N-1)\sum_{i \in I_1} d_i^{-\gamma} = \sum_{i \in I_0} d_i^{-\gamma}. \tag{30}$$

For the 19-cell model with parameters $N = 2$ and $r = 1$, (30) becomes

$$\frac{1}{d_2^{\gamma}} = \sum_{i=3}^{19} \frac{1}{d_i^{\gamma}}. \tag{31}$$

It can be numerically verified that (31) holds near $d = 0.73$, which is the normalized distance value at which the SINR curves for MRC and ZF-ISD cross in Fig. 4.

Although the effective SINR always increases as reuse factor r decreases due to the reduced amount of interference, a similar trend does not always hold for the capacity which is normalized by the reuse factor. Figure 6 shows the evaluation result of the capacity formulas in (12), (24), and (28) for different values of normalized distance d. It is indicated that the full reuse maximizes the capacity for small values of d, whereas a partial reuse yields an improved spectral efficiency as the MS moves toward the cell boundary. More specifically, the maximum spectral efficiency is achieved by frequency reuse $r = 1$ for inner cell users at $d < 0.71$ and by frequency reuse $r = 2/3$ for outer cell users at $d > 0.71$ performing the MMSE-ISD detection. This important observation gives the motivation for the system-level interference coordination using dynamic frequency reuse, com-

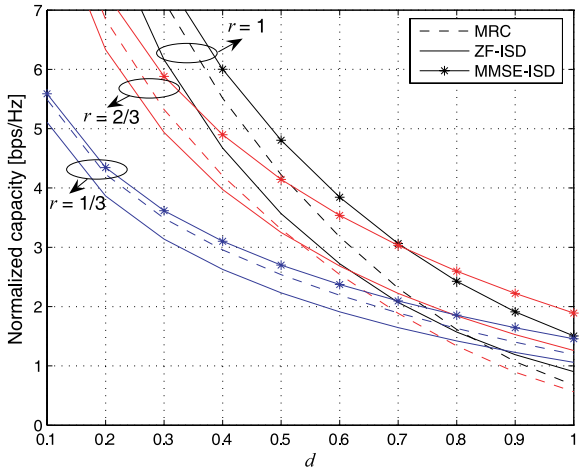

Fig. 6. Location-wise capacity using MRC, ZF-ISD, and MMSE-ISD for reuse factors $r = 1$, $2/3$, and $1/3$.

bined with the MMSE-ISD reception at the MS. The analytic results given in this section are also confirmed by experiments based on AMC transmission.

IV. SPECTRAL EFFICIENCY USING AMC

For more practical performance evaluation, signal transmission and reception using the link adaptation with AMC is performed using the system parameters shown in Table 1. The parameters are per IEEE802.16e [2],[3] utilizing the 10 MHz bandwidth with 867 used subcarriers. M-QAM modulation schemes with constellation sizes 4, 16, and 64 (or equivalently 2^q-QAM with modulation indices $q = 2$, 4, and 6) combined with different coding rates R constitute 10 modulation and coding selection (MCS) levels. Based on the instantaneous link quality determined from the desired and interference signals transmitted over time-varying Rayleigh fading channels, the MCS level is chosen using *exponential effective SINR mapping* (EESM) [1] with 1% target frame error rate (FER). The average bandwidth efficiency at normalized distance d with frequency reuse r is calculated from repeated random generations of the channel profiles as

$$\bar{S}(d) = r \cdot \sum_{k=1}^{10} S_k P_k(d) \tag{32}$$

where S_k is the bandwidth efficiency $q \cdot R$ of the kth MCS level in bits per symbol, and $P_k(d)$ is the occurrence probability of the kth MCS level at d. For the simulation, the MS locations are uniformly distributed on the ring with its radius equal to d as shown in Fig. 3.

The evaluation results for the average spectral efficiency using the MRC, ZF-ISD, and MMSE-ISD detection with reuse factors $r = 1$, $2/3$, and $1/3$ are summarized in Fig. 7, indicating resemblance to analytic capacity values in Fig. 6 in their general trends. Again the maximum spectral efficiency is achieved by the full reuse $r = 1$ by inner cell users ($d < 0.7$), and by reuse $r = 2/3$ by outer cell users ($d > 0.7$) with the MMSE-ISD detection. Also shown in the figure is the spectral efficiency

Table 1. Simulation Parameters.

Parameters	Value
System bandwidth	10 MHz
OFDM symbol duration	102.4 ms (w/o cyclic prefix)
# of used subcarriers	867
Channel model	Flat fading
Channel coding	Convolutional code ($K = 7$)
Link	Downlink
MCS level	QPSK: $R = 1/12, 1/8, 1/4, 1/2, 3/4$ 16QAM: $R = 1/2, 3/4$ 64QAM: $R = 1/2, 2/3, 3/4$
Antenna configuration	1-Tx BS / 2-Rx MS
Channel estimation	Perfect CSI at MS, no CSI at BS
Cell configuration	19 cells
BS-to-BS distance	2 km
Pathloss exponent	3.76
Total BS power	43 dBm
Thermal noise level	-174 dBm/Hz

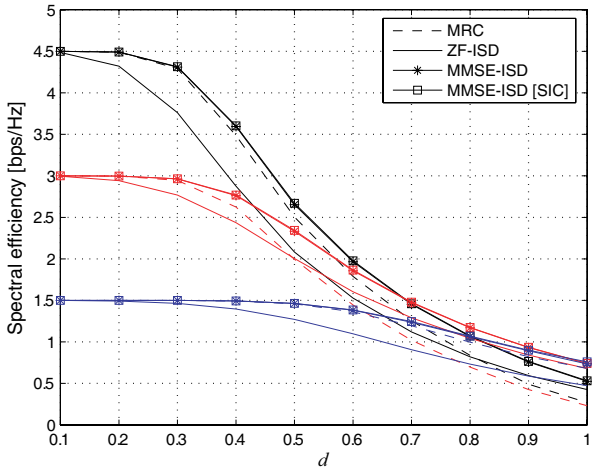

Fig. 7. Location-wise spectral efficiency using MRC, ZF-ISD, and MMSE-ISD with AMC transmission.

obtained by using the MMSE-ISD with successive interference cancellation (SIC). We observe that virtually no additional gain is obtained by performing SIC, since the desired data stream has the strongest received power in most of the region and detected first when the SIC algorithm is applied.

The performance advantage of ISD is also demonstrated by the distribution of the MCS levels in Fig. 8, where the occurrence probabilities $P_k(1)$ and $P_k(0.7)$ are shown and compared with the similar distribution for the MRC detection. The distributions for ISD with $r = 2/3$ are substantially shifted to the right, compared to those for MRC with $r = 1$. This suggests that higher MCS levels are selected for ISD, both at $d = 0.7$ (near cross-over point) and $d = 1$ (extreme cell edge). Thus even with the normalization by the resource usage factor r, ISD exhibits an improved spectral efficiency near the cell edge. As shown in

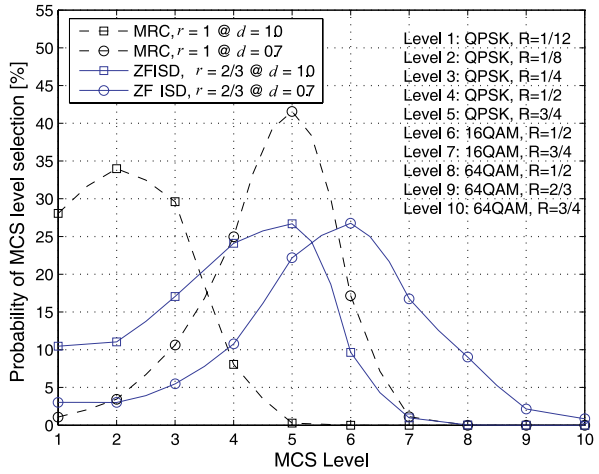

Fig. 8. MCS level occurrence probabilities for MRC with $r = 1$ and ISD with $r = 2/3$.

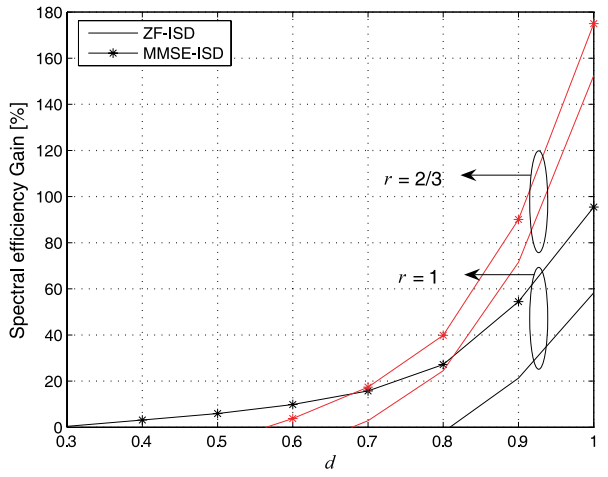

Fig. 9. Spectral efficiency gain of ISD with $r = 2/3$ and $r = 1$ over MRC with $r = 1$.

Fig. 9, the spectral efficiency gain by using ISD detection with $r = 2/3$ and $r = 1$ compared to MRC with $r = 1$ monotonically increases as d increases, and performance gain by using MMSE-ISD detection with $r = 2/3$ is increasing up to 170% gain at $d = 1$.

Using the performance evaluation results, we conclude that an effective strategy for spectral efficiency enhancement is to employ an adaptive scheme for signal transmission, in conjunction with the MMSE-ISD detection at the receiver. Dynamic FFR with two reuse factors $r = 1$ for inner cell users and $r = 2/3$ for outer cell users is desired, as shown in Fig. 10(a). Note that this type of adaptation is signal quality based, hence a fixed geometric boundary between two reuse factors may not firmly exist as in Fig. 10(a), which is drawn for an illustration purpose. Also, the partition of the bandwidth for each frequency block illustrated in Fig. 10(c) needs to be determined by considering traffic distributions within a cell as well as various QoS requirements.

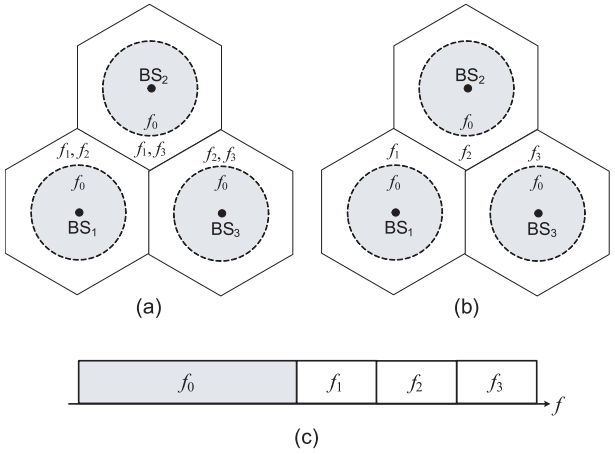

Fig. 10. Illustration of the resource allocation for dynamic FFR: (a) Usage of two frequency reuse factors $r = 1$ and $r = 2/3$, (b) usage of two frequency reuse factors $r = 1$ and $r = 1/3$, and (c) channelization of the bandwidth.

V. PRACTICAL CONSIDERATIONS AND DISCUSSION

A. Traffic Loading

Suppose at a particular time instance, the system is operated with traffic loading factor of β ($0 \leq \beta \leq 1$). For example, $\beta = 0.5$ represents 50% of the bandwidth resource is being utilized. As β decreases from the fully loaded case of $\beta = 1$, the co-channel interference reduction occurs and the system essentially resembles the case of using a reduced frequency reuse factor. Thus the loading variation can be regarded as the reuse factor change, and the combined effect of traffic loading and frequency reuse on the performance needs to be identified.

Fig. 11 shows the average spectral efficiency of AMC for uniformly distributed users in the outer cell region ($0.7 \leq d \leq 1$), using different values of β. The spectral efficiency curves plotted in the figure are obtained by multiplying β to the expression given in (32), to reflect the efficiency over the entire usable bandwidth. It can be observed that the maximum efficiency is achieved by MMSE-ISD with $r = 2/3$ when the loading is high ($\beta > 0.57$). For the low loading case ($\beta < 0.57$), MMSE-ISD with $r = 1$ exhibits the maximum efficiency. Since a reduced amount of interference exists when loading is low, the detection capability of ISD can be efficiently exploited with the full frequency reuse. Thus over the entire traffic loading conditions, MMSE-ISD outperforms MRC with a noticeable difference in spectral efficiency. From this observation, the dynamic FFR strategy can further be adjusted when traffic loading is expected to vary, i.e., to use $r = 1$ is for all users regardless of the location when loading is low.

B. Channel Estimation Errors

An important consideration in determining the receiver performance is its sensitivity to channel estimation errors. Since ISD detection requires the estimation of the channel using the signals transmitted from multiple BS's, the estimation perfor-

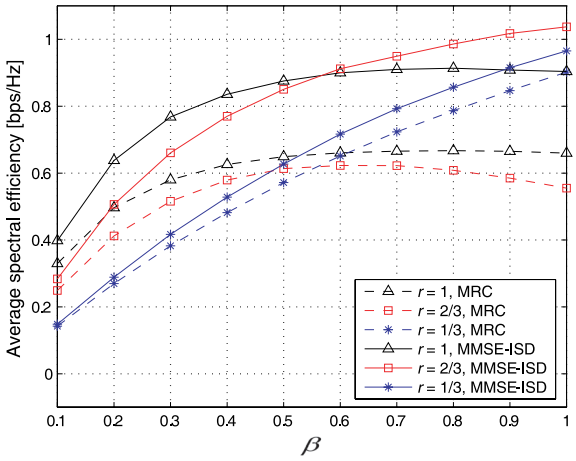

Fig. 11. Average spectral efficiency over the distance range $d = [0.7, 1.0]$.

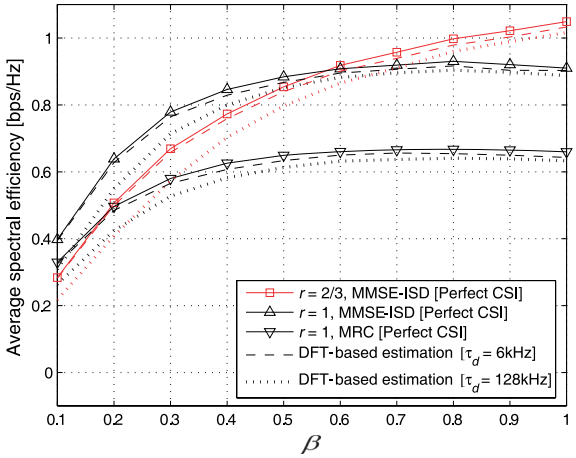

Fig. 12. Average spectral efficiency over the range $d = [0.7, 1.0]$, with channel estimation errors.

mance and its impact on the overall efficiency needs to be investigated. For the performance investigation, PUSC symbols [3] are used for the data transmission, and the preamble symbol with three disjoint sets of pilot locations is used for the multicell channel estimation. For each set, 283 pilot subcarriers are located in modulo-3 positions and multiplied by one of 57 distinct pseudo-random sequences. Due to the disjoint structure, the estimation error caused by the signals from adjacent cells can be minimized, and the signals from the cells using the same modulo-3 positions can be further differentiated with the aid of the pseudo-random sequence.

Using this preamble and the DFT-based channel estimation method [28], the MRC and MMSE-ISD detection is performed and corresponding spectral efficiency curves for several cases of interest are plotted in Fig. 12, which also includes some of the curves from Fig. 11 representing the performance with ideal channel state information (CSI) for comparison. The Doppler frequency values of 6 Hz and 128 Hz, which respectively correspond to vehicular speeds of 3 km/h and 60 km/h with 2.3 GHz center frequency are used for the performance evaluation. While marginal performance loss is shown for 6 Hz, performance degradation increases at 128 Hz Doppler frequency. Nevertheless, the general behavior of the efficiency curves remains unchanged after channel estimation is performed, for both the MRC and ISD detection.

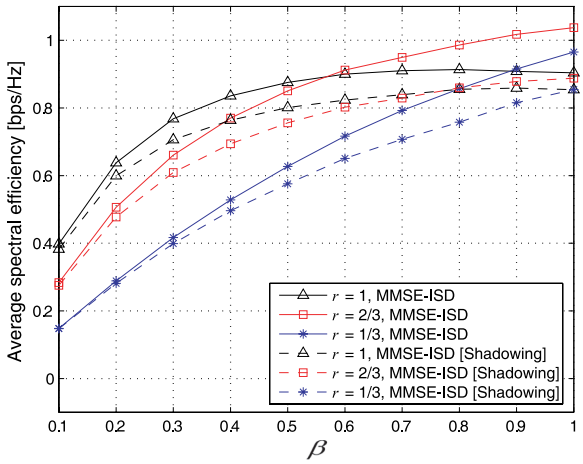

Fig. 13. Average spectral efficiency over the range $d = [0.7, 1.0]$, with the effect of shadowing.

C. Effect of Shadowing

The shadowing effect in wireless channels often causes a severe degradation in performance. To verify the performance of the detection schemes in consideration, we model the shadowing parameter $\{L_i\}$ in (1) as independent log-normal random variables with zero mean and standard deviation of 8.9 dB, as suggested in [1]. The evaluation results are shown in Fig. 13, which also includes the performance without shadowing effect for comparison. The spectral efficiency reduces due to shadowing effects for all considered cases, and the amount of degradation is shown to increase for larger values of traffic loading β. It is again observed that the maximum efficiency is achieved by MMSE-ISD with $r = 2/3$ for high loading, and by MMSE-ISD with $r = 1$ for low loading as before, but the distinction between high and low loading has shifted to $\beta = 0.75$ under this channel condition, compared to $\beta = 0.57$ for the channel without shadowing.

D. Generalization to Multi-Antenna Transmission

For MIMO transmission in cellular environment, transmission methods with a reduced spatial rate such as space-time coding (STC) [29] and cyclic delay diversity (CDD) [30] are usually employed for users experiencing low SINR, for improved performance over spatial multiplexing (SM). Due to the simple receiver structure, CDD has recently been adopted as a transmission method in 3GPP-LTE standard [31]. When such reduced-rate transmission is used, the proposed scheme performing adaptive reception can also be applied to general MIMO systems

with multi-antenna BS's. Suppose, for example, a dual-antenna MS receives signals from two dual-antenna BS's with rate-1 transmission near the cell boundary. Since the situation is essentially identical to transmission by two single-antenna BS's in terms of the number of data streams, MS can perform a similar ISD operation to separate the desired signal from the interfering signals.

Experimental results using the same transmission parameters and the 19-cell configuration reveals the obtained spectral efficiency values have the similar trend, i.e., MMSE-ISD with $r = 1$ is the preferred mode of operation for inner cell users and MMSE-ISD with $r = 2/3$ is the preferred mode of operation for outer cell users, with the spectral efficiency cross-over occurring at normalized distance $d = 0.71$.

VI. CONCLUSIONS

We demonstrated the ISD detection in conjunction with appropriate frequency reuse factors can provide an enhanced spectral efficiency for receivers under the influence of co-channel interference. In particular, ISD utilizing the MMSE algorithm achieves a significant performance improvement over the conventional MRC detection. As the amount of traffic loading changes, a cooperative resource usage among transmitters are required; from the performance evaluation, reuse factors of 2/3 and 1 are respectively suggested for high and low loading conditions for the optimal performance. For the entire range of traffic loading and under various channel conditions, proposed MMSE-ISD combined with FFR is shown to provide improved receiver performance, enhancing the spectral efficiency near the cell coverage boundaries. The proposed scheme is applicable to systems with conventional single-antenna BS's, as well as multi-antenna BS's transmitting signals with a reduced spatial rate.

ACKNOWLEDGMENTS

This work has been supported in part by the Mobile Communication Technology R&D Center, LG Electronics, Inc, and in part by the Special Research Grant of Sogang University.

REFERENCES

[1] WiMAX Forum, *WiMAX System Evaluation Methodology*, V0.8, Oct. 2006.

[2] Institute of Electrical and Electronics Engineers, Inc., *IEEE Standard for Local and Metropolitan Area Networks, Part 16: Air Interface for Fixed Broadband Wireless Access Systems*, IEEE Std 802.16-2004, New York, USA, Oct. 2004.

[3] Institute of Electrical and Electronics Engineers, Inc., *IEEE Standard for Local and metropolitan area networks, Part 16: Air Interface for Fixed Broadband Wireless Access Systems*, IEEE Std 802.16e-2005, New York, USA, Feb. 2006.

[4] H. M. Sachs, "A realistic approach to defining the probability of meeting acceptable receiver performance criteria," *IEEE Trans. Electromagn. Compaf.*, vol. 13, Nov. 1971, pp. 3–6.

[5] R. C. French, "The effect of fading and shadowing on channel reuse in mobile radio," *IEEE Trans. Veh. Technol.*, vol. 28, pp. 171–181, Aug. 1979.

[6] H. Sato, "The capacity of the Gaussian interference channel under strong interference," *IEEE Trans. Inf. Theory*, vol. 27, pp. 786–788, Apr. 1981.

[7] Y. S. Yeh and S. C. Schwartz, "Outage probability in mobile telephony due to multiple log-normal interferers," *IEEE Trans. Commun.*, vol. 32, pp. 380–387, Apr. 1984.

[8] A. G. Williamson and J. D. Parsons, "Outage probability in a mobile radio system subject to fading and shadowing," *Electron. Lett.*, vol. 21, pp. 622–623, 1985.

[9] K. W. Sowerhy and A. G. Williamson, "Outage probability calculations for mobile radio systems with multiple interferers," *Electron. Lett.*, vol. 24, pp. 1073–1075, 1988.

[10] V. P. Mhatre and C. P. Rosenberg, "Impact of network load on forword link inter-cell interference in cellular data networks," *IEEE Trans. Wireless Commun.*, vol. 5, pp. 3651–3660, Dec. 2006.

[11] J. H. Winters, "Optimum combining in digital mobile radio with cochannel interference," *IEEE J. Sel. Areas Commun.*, vol. 2, pp. 528–539, July 1984.

[12] D. C. Cox and D. O. Reudink, "Dynamic channel assignment in high capacity mobile communications systems," *Bell Syst. Tech. J.*, July/Aug. 1971.

[13] D. C. Cox and D. O. Reudink, "A comparison of some channel assignment strategies in large-scale mobile communications systems," *IEEE Trans. Commun.*, vol. 20, pp. 190–195, Apr. 1972.

[14] I. Katzela and M. Naghshineh, "Channel assignment schemes for cellular mobile telecommunication systems: A comprehensive survey," *IEEE Pers. Commun.*, vol. 3, pp. 10–31, June 1996.

[15] IEEE 802.20 working group on mobile broadband wireless access, *MBFDD and MBTDD wideband mode: Technology overview*, IEEE C802.20-05/68r1, New York, USA, Jan. 2006.

[16] Z. Xu, A. N. Akansu, and S. Tekinay, "Cochannel interference computation and asymptotic performance analysis in TDMA/FDMA systems with interference adaptive dynamic channel allocation," *IEEE Trans. Veh. Technol.*, vol. 49, no. 3, pp. 711–723, May 2000.

[17] X. Wang and J. Wang, "Effect of imperfect channel estimation on transmit diversity in CDMA systems," *IEEE Trans. Veh. Technol.*, vol. 53, no. 5, pp. 1400–1412, Sept. 2004.

[18] A. B. Gershman and N. D. Sidiropoulos, *Space-Time Processing for MIMO Communications*. New York: Wiley, 2005.

[19] D. G. Brennan, "Linear diversity combining techniques," *Proc. IEEE*, vol. 91, pp. 331–356, Feb. 2003.

[20] J. G. Proakis, *Digital communications*, 3rd ed. New York: McGraw-Hill, 1995.

[21] A. J. Paulraj, D. A. Gore, R. U. Nabar, and H. Bolcskei, "An overview of MIMO communications: A key to gigabit wireless," *Proc. IEEE*, vol. 92, pp. 198–218, Feb. 2004.

[22] G. J. Foschini, G. D. Golden, R. A. Valenzuela, and P. W. Wolniansky, "Simplified processing for high spectral efficiency wireless communication employing multi-element arrays," *IEEE J. Sel. Areas Commun.*, vol. 17, pp. 1841–1852, Nov. 1999.

[23] A. Zanella, M. Chiani, and M. Z. Win, "MMSE reception and successive interference cancellation for MIMO systems with high spectral efficiency," *IEEE Trans. Wireless Commun.*, vol. 4, pp. 1244–1253, May 2005.

[24] G. D. Golden, C. J. Foschini, R. A. Valenzuela, and P. W. Wolniansky, "Detection algorithm and initial laboratory results using V-BLAST space-time communication architecture," *Electron. Lett.*, vol. 35, pp. 14–16, Jan. 1999.

[25] S. Catreux, P. F. Driessen, and L. J. Greenstein, "Data throughputs using multiple-input multiple-output (MIMO) techniques in a noise-limited cellular environment," *IEEE Trans. Wireless Commun.*, vol. 1, pp. 226–235, Apr. 2002.

[26] Y. Tokgoz, B. Rao, M. Wengler, and B. Judson, "Performance analysis of optimum combining in antenna array systems with multiple interferers in flat Rayleigh fading," *IEEE Trans. Commun.*, vol. 52, pp. 1047–1050, July 2004.

[27] 3GPP TR 25.892, *Feasibility Study for Orthogonal Frequency Division Multiplexing for UTRAN Enhancement*, V2.0.0, June 2004.

[28] Y. Zhao and A. Huang "A novel channel estimation method for OFDM mobile communication systems based on pilot signals and transform-domain processing," in *Proc. IEEE VTC*, vol. 3, May 1997, pp. 2089–2093.

[29] S. M. Alamouti, "A simple transmitter diversity technique for wireless communication," *IEEE J. Sel. Areas Commun.*, vol. 16, pp. 1451–1458, Oct. 1998.

[30] Z. Hong, L. Zhang, and L. Thibault, "Performance of cyclic delay diversity in DAB/DMB," *IEEE Trans. Broadcast.*, vol. 52, pp. 318–324, Sept. 2006.

[31] 3rd Generation Partnership Project, *Technical specification Group Radio Access Network, Evolved Universal Terrestrial Radio Access (E-UTRA); Physical channels and modulation*, 3GPP TS 36.211 V8.0.0, Sept. 2007.

[32] W. C. Jakes, *Microwave Mobile Communication*, 2nd ed. Piscataway, NJ: IEEE Press, 1994.

[33] T. K. Y. Lo, "Maximum ratio transmission," *IEEE Trans. Commun.*, vol. 47, pp. 1458–1461, Oct. 1999.

[34] B. D. Rao and M. Yan, "Performance analysis of maximal ratio trans-

mission with two receive antennas," *IEEE Trans. Commun.*, vol. 51, pp. 894–895, June 2003.
[35] R. W. Heath Jr. and A. J. Paulraj, "Switching between diversity and multiplexing in MIMO systems," *IEEE Trans. Commun.*, vol. 53, June 2005, pp. 962–968.
[36] W. Zhi, F. Chin, and C. C. Ko, "Capacity comparison of multi-element antenna systems," in *Proc. IEEE VTC*, vol. 1, Apr. 2003, pp. 85–88.
[37] P. Li, R. Narasimhan and J. Cioffi, "On the distribution of SINR for the MMSE MIMO receiver and performance analysis," *IEEE Trans. Inf. Theory*, vol. 52, pp. 271–286, Jan. 2006.
[38] P. W. Wolniansky, G. J. Foschini, G. D. Golden, and R. A. Valenzuela, "V-BLAST: An architecture for realizing very high data rates over the rich-scattering wireless channel," in *Proc. IEEE ISSSE*, Sept. 1998, pp. 295–300.
[39] J. Zhu, G. Liu, Y. Wang, and P. Zhang, "A hybrid inter-cell interference mitigation scheme for OFDMA based E-UTRA downlink," in *Proc. APCC*, Aug. 2006, pp. 1–5.
[40] M. Vemula, D. Avidor, J. Ling, and C. Papadias, "Inter-cell coordination, opportunistic beamforming and scheduling," in *Proc. IEEE ICC*, vol. 12, June 2006, pp. 5319–5324.

Jaewon Chang received the B.S. and M.S. degrees in Electronic Engineering from Sogang University, Seoul, Korea, in 2003 and 2005, respectively. From February 2005 through March 2007, he worked at LG Electronics, Inc., Seoul, Korea, where he was a Research Engineer responsible for the multiple-antenna technology development and related standard activities for the IEEE802.16e and 3GPP LTE systems. Since March 2007, he has been working toward his Ph.D. degree at Sogang University. His current research interests include MIMO, OFDM, communications theory, and distributed antenna systems.

Jun Heo received the B.S. and M.S. degrees in Electronics Engineering from Seoul National University, Seoul, Korea in 1989 and 1991, respectively and the Ph.D. degree in Electrical Engineering from the University of Southern California, Los Angeles, USA in 2002. From 1991 to 1997, he was a Senior Research Engineer at LG Electronics, Inc. From 2003 to 2006, he was an assistant professor in the Electronics Engineering Department, Konkuk University, Seoul, Korea. He is presently an assistant professor in the School of Electrical Engineering at Korea University, Seoul, Korea. His research interests include channel coding theory and digital communication systems.

Wonjin Sung received his B.S. degree from Seoul National University, Korea in 1990, and the M.S. and Ph.D. degrees in Electrical Engineering from University of Michigan, Ann Arbor, MI, in 1992 and 1995, respectively. From January 1996 through August 2000, he worked at Hughes Network Systems, Germantown, MD, USA, where he participated in development projects for cellular and satellite systems including base station modems for the IS-136 North American TDMA, multi-mode terminals for medium orbit satellites, and the Inmarsat air interface design. Since September 2000, he has been with the Department of Electronic Engineering at Sogang University, Seoul, Korea, where he is currently an associate professor. His research interests are in the areas of mobile wireless transmission, statistical communication theory, distributed antenna systems, and satellite modems.